Draft version June 12, 2025
Typeset using LaTeX twocolumn style in AASTeX631

An upper limit of $10^6\,M_\odot$ in dust from ALMA observations in 60 Little Red Dots

Caitlin M. Casey,[1,2] Hollis B. Akins,[3,*] Steven L. Finkelstein,[3] Maximilien Franco,[4] Seiji Fujimoto,[3,†] Daizhong Liu,[5] Arianna S. Long,[6] Georgios Magdis,[2,7,8] Sinclaire M. Manning,[9,‡] Jed McKinney,[3,‡] Marko Shuntov,[2,8] and Takumi S. Tanaka[10,11,12]

[1] *Department of Physics, University of California, Santa Barbara, Santa Barbara, CA 93106, USA*
[2] *Cosmic Dawn Center (DAWN), Denmark*
[3] *Department of Astronomy, The University of Texas at Austin, 2515 Speedway Blvd Stop C1400, Austin, TX 78712, USA*
[4] *Université Paris-Saclay, Université Paris Cité, CEA, CNRS, AIM, 91191 Gif-sur-Yvette, France*
[5] *Purple Mountain Observatory, Chinese Academy of Sciences, 10 Yuanhua Road, Nanjing 210023, China*
[6] *Department of Astronomy, The University of Washington, Seattle, WA 98195, USA*
[7] *DTU-Space, Technical University of Denmark, Elektrovej 327, 2800, Kgs. Lyngby, Denmark*
[8] *Niels Bohr Institute, University of Copenhagen, Jagtvej 128, DK-2200, Copenhagen, Denmark*
[9] *Department of Astronomy, University of Massachusetts Amherst, MA 01003, USA*
[10] *Department of Astronomy, Graduate School of Science, The University of Tokyo, 7-3-1 Hongo, Bunkyo-ku, Tokyo, 113-0033, Japan*
[11] *Kavli Institute for the Physics and Mathematics of the Universe (WPI), The University of Tokyo Institutes for Advanced Study, The University of Tokyo, Kashiwa, Chiba 277-8583, Japan*
[12] *Center for Data-Driven Discovery, Kavli IPMU (WPI), UTIAS, The University of Tokyo, Kashiwa, Chiba 277-8583, Japan*

ABSTRACT

By virtue of their red color, the dust in little red dots (LRDs) has been thought to be of appreciable influence, whether that dust is distributed in a torus around a compact active galactic nucleus (AGN) or diffuse in the interstellar medium (ISM) of nascent galaxies. In Casey et al. (2024) we predicted that, based on the compact sizes of LRDs (unresolved in *JWST* NIRCam imaging), detection of an appreciable dust mass would be unlikely. Here we present follow-up ALMA 1.3 mm continuum observations of a sample of 60 LRDs drawn from Akins et al. (2024). None of the 60 LRDs are detected in imaging that reaches an average depth of $\sigma_{\rm rms} = 22\,\mu$Jy. A stack of the 60 LRDs also results in a non-detection, with an inverse-variance weighted flux density measurement of $S_{\rm 1.3mm}$ =2.1±2.9 μJy. This observed limit translates to a 3σ upper limit of 10^6 $M_\odot$ in LRDs' dust mass, and $\lesssim 10^{11}$ $L_\odot$ in total dust luminosity; both are a factor of 10× deeper than previous submm stack limits for LRDs. These results are consistent with either the interpretation that LRDs are reddened due to compact but modest dust reservoirs (with $A_V \sim 2-4$) or, alternatively, that instead of being reddened by dust, they have extreme Balmer breaks generated by dense gas ($> 10^9\,{\rm cm}^{-3}$) enshrouding a central black hole.

1. INTRODUCTION

The discovery of little red dots (LRDs) by JWST has been a perplexing mystery. Characterized by compact (unresolved) morphologies and red rest-frame optical colors (sometimes with a faint, blue component in the rest-frame UV, giving a 'V-shaped' SED; Labbe et al. 2022, 2023; Kokorev et al. 2024; Kocevski et al. 2024), the population of LRDs at $z > 5$ is surprisingly ubiquitous, with volume densities $\gtrsim 10^{-5}$ Mpc^{-3}, making up a few percent of the galaxy population at these epochs. And yet, a similar population at low-z ($z < 3$) LRDs – both compact and red – seem to be far more rare (Lin et al. 2025a; Bisigello et al. 2025; Ma et al. 2025).

Spectral follow-up efforts have revealed the ubiquity of luminous active galactic nuclei (AGN) among the LRD population (Matthee et al. 2024; Greene et al. 2023; Taylor et al. 2024). Though the detection of a Balmer break in some LRDs has led to a hypothesis that LRDs are not dominated by light from AGN (Wang et al. 2024), assuming they are comprised of highly compact and old stellar populations proves problematic in a number of

Corresponding author: Caitlin M. Casey
cmcasey@ucsb.edu

* NSF Graduate Research Fellow
† Hubble Fellow
‡ NASA Hubble Fellow

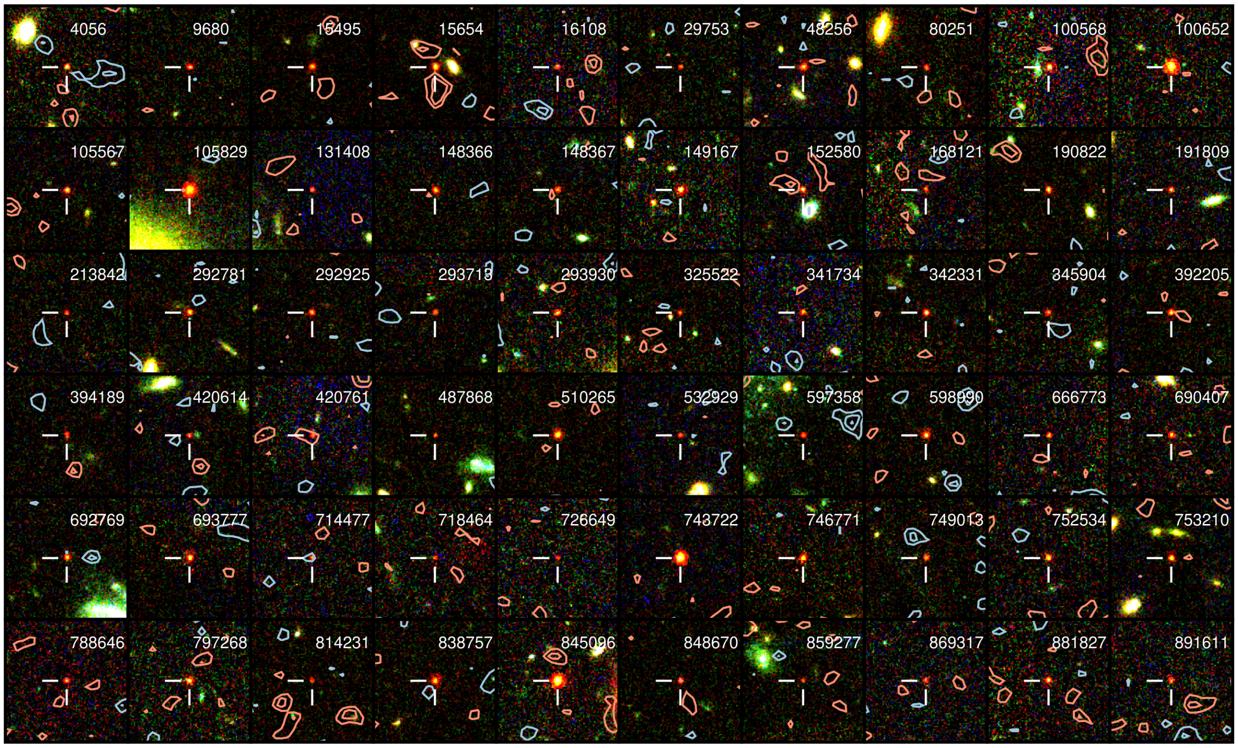

Figure 1. JWST 5″×5″ tricolor cutouts (F150W, F277W, F444W) of our LRD sample overlaid with ALMA dust continuum contours. Blue contours denote positive SNR (integer multiples of σ beginning at 2σ) and red contours denote negative SNR (integer multiples of σ descending from -2σ). None of the 60 LRDs in this program were detected with 1σ RMS ranging 21-23 μJy.

ways – they are excessively dense (Baggen et al. 2024) and push the limits of stellar mass assembly at early times if so (Williams et al. 2023). Alternatively, Inayoshi & Maiolino (2024) posit that LRDs are caused by very dense ($>10^9\,\mathrm{cm}^{-3}$) neutral hydrogen surrounding the accretion disk of an AGN. This idea is supported by recent observations of LRDs with extreme Balmer break strengths, exceeding the maximal expected from a stellar population (Naidu et al. 2025; Rusakov et al. 2025; de Graaff et al. 2025; Ji et al. 2025; Taylor et al. 2025).

Whether or not the rest-frame optical emission is dominated by compact stellar populations or AGN, the red nature of the population has naturally led to the hypothesis that LRDs are dust-obscured[1]. Significant obscuration (implied $A_V \sim 2-4$) may suggest substantial dust reservoirs obscuring their light on ∼10's or ∼100's of parsecs. Labbe et al. (2022) and Akins et al. (2024) present some of the first limits on dust content of LRDs from pre-existing submm datasets in the deep fields in which their LRDs are found. No LRDs were detected in those datasets among hundreds, though their limits were not particularly sensitive to masses $<10^7$ M$_\odot$ (with stacked upper limits of order $S_{1.2\mathrm{mm}}$ <0.1 mJy at 5σ). Recently, deep NOEMA observations of two $z>7$ LRDs (Xiao et al. 2025) and separately, multi-band ALMA observations of two of the brightest LRDs known (Setton et al. 2025) result in more stringent non-detections.

In Casey et al. (2024) we present the prediction that LRDs' dust masses are limited to $\sim10^{4-5}$ M$_\odot$, with their compact sizes primarily driving significant attenuation at relatively low mass. This was primarily based on earlier submm limits (and in agreement with the more recent results of Xiao et al. 2025 and Setton et al. 2025). If LRDs were more dust-rich, then they would have already presented as detections in the submillimeter or at least show some highly obscured but detectable extended host-galaxy emission in NIRCam imaging.

[1] Though we note that the Inayoshi & Maiolino (2024) argument for a black hole enshrouded in dense gas does not explicitly require *any* dust obscuration, and super-Eddington accretion onto black holes may naturally lead to a redder continuum (Lambrides et al. 2024; Quadri et al. 2025; Madau 2025).

In this work we present new ALMA 1.3 mm continuum follow-up observations of a large sample of 60 bright LRDs at $z \sim 5-8$ selected from Akins et al. (2024) to search for anomalously large dust reservoirs $\gtrsim 10^6$ M$_\odot$ at $\lesssim$100 K temperatures. This constitutes the largest sample of LRDs for which deep dust continuum measurements have been made. Section 2 presents the LRD sample, ancillary data and ALMA observations, section 3 presents the measurements, and section 4 discusses the implications of the new limits. Throughout we adopt a Planck cosmology (Planck Collaboration et al. 2020), AB magnitudes (Oke & Gunn 1983) and a Chabrier initial mass function (IMF; Chabrier 2003).

2. SAMPLE SELECTION & OBSERVATIONS

We select LRDs for ALMA observations from the COSMOS-Web (Casey et al. 2023) sample of LRDs (Akins et al. 2024). COSMOS-Web covers more than three times the area of all other JWST deep fields combined so is particularly sensitive to the rarest, brightest sources. These are arguably the most likely LRDs to exhibit a dust detection. A third of the field is also covered by MIRI 7.7μm imaging, giving further direct constraints on the rest-frame NIR of the LRD population.

The LRD selection in Akins et al. (2024) can be summarized as (a) a compactness cut, such that sources are unresolved in F444W, (b) very red color in NIRCam LW filters, such that $m_{277} - m_{444} > 1.5$, and (c) lack of good fit to brown dwarf templates. It does not explicitly require a "V-shaped" SED in the rest-UV; this choice was jointly motivated by the lack of understanding of the physics generating the UV emission and if it is related to the red rest-optical and depth limitations in COSMOS-Web SW imaging. While some may be concerned that the lack of blue rest-frame UV requirement or sparse filter coverage in COSMOS-Web leaves us more prone to contamination from, e.g., extreme emission line galaxies, compared to smaller deep fields with more extensive NIRCam coverage, this concern is directly addressed by the *very* red selection in [F277W]-[F444W]. The strength of that drop greatly reduces possible contaminants; the addition of MIRI detection at 7.7 μm further refines the photometric redshifts of the sample so they have similar uncertainties as what one might generate using a tight detection of a Lyman-break in the rest-UV. Though a small subset, some of the Akins et al. (2024) LRDs have already been spectroscopically confirmed as broad-line AGN from the COSMOS-3D program (Lin et al. 2025b), demonstrating a high purity for this LRD photometric selection in COSMOS-Web.

Of the several hundred LRDs found in COSMOS-Web, we select a subset with the most potential for large dust reservoirs: those that are reddest (i.e. dustiest, as measured directly via color and through derived A$_V$ from SED fitting) and the brightest. Of the 148 LRDs presented in Akins et al. (2024) with MIRI F770W imaging, we apply the following specific criteria to select a subset for ALMA observations:

- [F444W]<27,
- [F770W]<26.5 with a detection $>5\sigma$, and
- [F277W] - [F444W]>1.7.

The first criterion selects bright LRDs. The second (MIRI) criterion is crucial for anchoring the long-wavelength SED of LRDs, providing direct evidence that the selected LRDs lack dominant mid-IR powerlaws (and are thus inconsistent with hot dust tori). Though these are MIRI detected, none of the selected sources have SEDs consistent with such a mid-IR powerlaw; the MIRI detections are also critical for ruling out brown dwarf contaminants. The red criterion maps directly to a high derived absolute magnitudes of attenuation $A_V > 2$ from SED fitting. Significant attenuation implies that this subset may have the highest potential to be the dustiest.

The above criteria result in the selection of a sample of 60 LRDs (about $\sim$40% of the original 148 MIRI-observed LRDs from Akins et al. 2024). Their photometric redshifts span $5 < z < 8$ (with a median $\langle z \rangle = 6.1$) and are well-constrained due to their red [F277W]-[F444W] color and MIRI detections. This sample size was motivated by the firm constraints it could set on the results, with a stacked uncertainty on the resulting flux density <5 μJy, translating to a dust mass uncertainty of 2×10^6 M$_\odot$ for assumed dust temperature $\sim$100 K.

ALMA observations were carried out in band 6 (1.3 mm) as part of project 2024.1.00708.S (PI: Casey) with 37.3 hours with the goal of achieving a 25 μJy beam^{-1} continuum RMS with $\sim$24 minutes on-source. Observations were split into four tunings to simultaneously search for serendipitous [CII] line emission in the $\sim$1/3 of the sample whose photometric redshifts would place [CII] in band 6. Three of the four tuning setups were executed covering frequencies 212–220 GHz, 224–236 GHz, and 240–244 GHz with a representative frequency 228 GHz (λ =1.316 mm). These frequencies cover redshift ranges z =6.78–6.91, z =7.05-7.48, and z =7.63-7.96 for the [CII] search. No obvious [CII] emitters were found, though we will be able to return to this data once spectroscopic redshifts are in hand to search for [CII] using an informed prior. Spectroscopic redshifts for many will come in the JWST Cycle 3 program

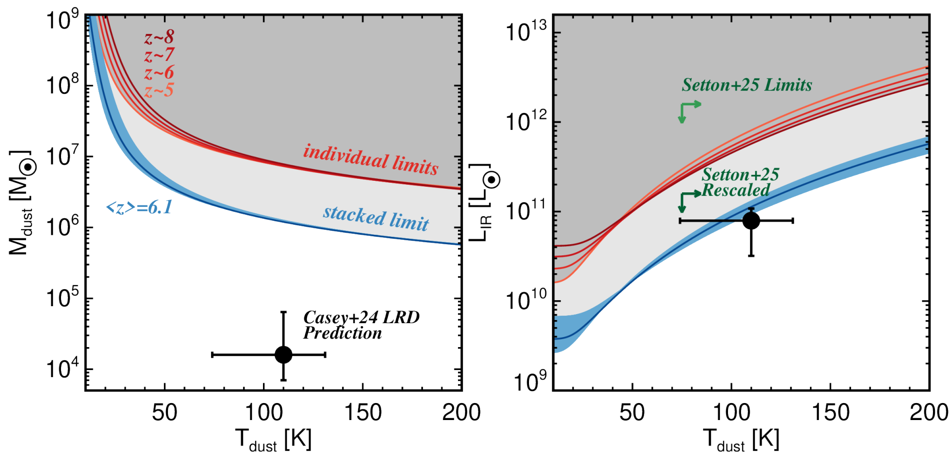

Figure 2. Limits we place on dust mass and IR luminosity based on our measurements as a function of dust temperature. The RMS per source ranges from 21–23 μJy at 1.3 mm, translating to a 3σ upper limit of 66 μJy; this sets an upper limit to the dust mass and IR luminosity of LRDs traced out by the red curves. We show the redshift dependence of this limit in different shades of red, from lightest ($z \sim 5$) to darkest ($z \sim 8$). The limited flux density for the stack, of 10.8 μJy at 3σ, is traced out by the blue line at the median redshift of the sample. We also show the measured limit to IR luminosity ($\lesssim 10^{12.2}$ L$_\odot$) and estimated dust temperature (>75 K) from Setton et al. (2025), derived from detailed ALMA and JWST/MIRI constraints on two very luminous LRDs (in green); their limits rescaled to the typical luminosity of our LRDs is shown in dark green. Despite uncertainty in the underlying dust temperature of the dust around LRDs, we place representative upper limits from these data of $< 10^7$ M$_\odot$ and $< 10^{12}$ L$_\odot$ on individual sources and $< 10^6$ M$_\odot$ and $< 10^{11}$ L$_\odot$ on the non-detection from the stack.

COSMOS-3D (# 5893, e.g. Lin et al. 2025b) and the Cycle 4 program EMBER (# 7076, PI: Akins).

Data were obtained spanning 11-Dec-2024 through 14-Jan-2025 and were reduced using the CASA pipeline version 6.6.1.17. The continuum sensitivity reaches per-source depths spanning $\sigma_{\rm rms} = 21.4$–$23.1\,\mu$Jy beam^{-1} with mean noise of $22.3\,\mu$Jy beam^{-1}. The synthesized beam averages to $0\farcs81\times0\farcs65$ using natural weighting.

3. DERIVED LIMITS ON DUST MASS

None of the 60 LRDs were detected in dust continuum. With typical RMS of 22 μJy, this gives a typical per-source 3σ (5σ) upper limit of $S_{1.3\,\rm mm}$ <67 μJy (<111 μJy). The measured SNR of each source's central unresolved beam ranges from –2.0 to 1.8, fully consistent with expectation from the null hypothesis, i.e. that none have discernible millimeter emission. The gallery of LRDs covered by this program are shown in Figure 1, with ALMA contours overlaying JWST tri-color images.

Beyond the non-detection of individual sources, we also stack our data in the image plane. This also results in a non-detection. The measured constraint on the flux density from the stack using inverse-variance weighting is $S_{1.3\,\rm mm} = 2.1 \pm 2.9\,\mu$Jy ($0.72\,\sigma$). We note this is not appreciably different from a direct, unweighted stack of $S_{1.3\,\rm mm} = 1.9 \pm 3.2\,\mu$Jy ($0.58\sigma$) because the RMS varies by less than 10% across the full sample.

Thanks to the negative K-correction, both dust mass and IR luminosity constraints derived from a single flux density measurement are largely insensitive to redshift. We calculate 3σ upper limits on dust masses in our sample by implementing Equation 1 of Casey et al. (2019), which is dust mass corrected for CMB heating. Because the LRDs span appreciably high redshifts $5 \lesssim z \lesssim 8$ the calculation of dust mass (or luminosity) requires accounting for the effect of CMB heating where the CMB temperature is non-negligible in the first 1 Gyr of cosmic time. CMB heating matters proportionally more for dust temperatures close to the CMB temperature, $T < 50$ K. Eq 1 of Casey et al. (2019) does require a number of adoptions: the dust mass absorption coefficient (for which we use the measurement at 450μm rest-frame of 1.3 ± 0.2 cm^2 g^{-1}; Li & Draine 2001), the dust emissivity index $\beta = 2$, and an assumption of the dominant temperature of the dust mass in LRDs. The temperature is the dominant source of uncertainty.

Figure 2 shows the temperature dependence of the dust mass limit and IR luminosity limit derived from our constraints on the 1.3 mm flux density of LRDs. Gray regions of parameter space are ruled out by our observations. Red curves show the typical 3σ upper limit per source where we use the representative $\sigma_{\rm rms} = 22\,\mu$Jy. Blue curves show the stacked limit of 10.8 μJy at 3σ for the full sample. Dust mass limits are largely insensitive to temperature above ∼50 K. Casey et al. (2024) present

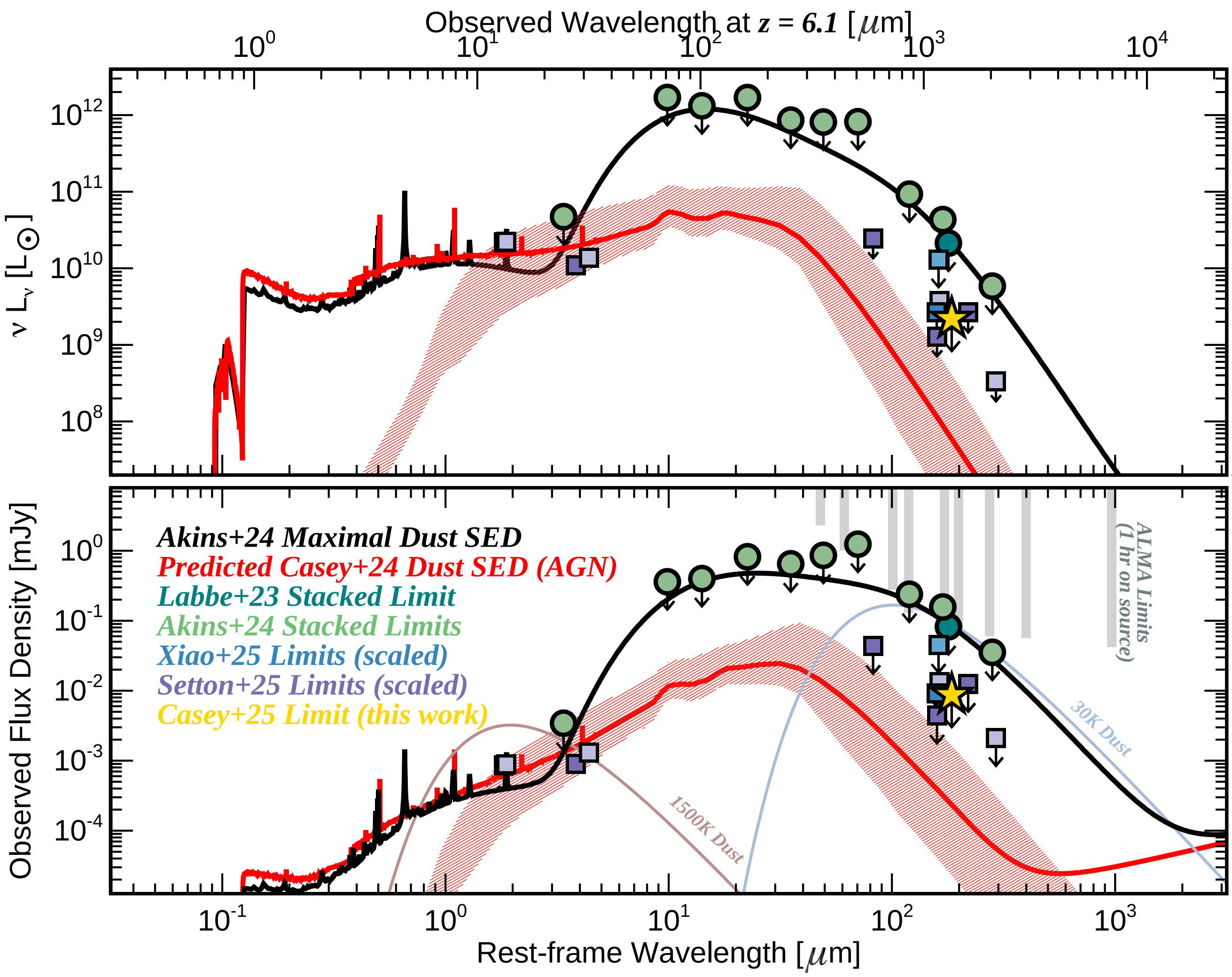

Figure 3. Our measured constraints on the stack of 60 LRDs (gold star) compared to other literature limits of dust emission around LRDs. The top panel plots the SED constraints in νL_ν and the bottom panel in observed flux density. Other limits from the literature are shown in dark teal (Labbe et al. 2022), light green (Akins et al. 2024), blue (Xiao et al. 2025), and purple (Setton et al. 2025). The Xiao et al. and Setton et al. limits are set for two different LRDs each: light blue represents ID9094 at $z = 7.0388$, dark blue is ID2756 at $z = 7.1883$, light purple is RUBIES-BLAGN-1 at $z = 3.1034$ and dark purple for A2744-45924 at $z = 4.4655$. Because these limits are all for unusually bright LRDs, we have scaled their limits down by a factor of 3, 10, 10, and 10 (respectively) to draw a more direct comparison to the LRDs targeted in our program. Two optical through radio SEDs are shown: the maximal SED from Akins et al. (2024), showing the maximum allowable dust SED around LRDs given the limits available (black), and the predicted LRD dust SED from Casey et al. (2024) in red. On the bottom panel we overplot simple modified black body SEDs with temperatures of 30 K and 1500 K for comparison. Our new limit for this aggregate sample is fully in line with the predicted low luminosity dust emission.

a discussion of why cold dust temperatures ($\lesssim$50 K) are not expected in LRDs given their compact morphologies. Note that an independent estimate of dust-heating by super-Eddington accreting AGN predicts temperatures $\sim$140 K (McKinney et al. 2021). Given the lack of strong temperature evolution on our derived limits above these temperatures, we quote the upper limit on dust mass of $< 10^7$ $M_\odot$ on individual sources and $< 10^6$ $M_\odot$ on the stack for the full sample.

We can similarly place limits on IR luminosity, though these are more temperature dependent than dust mass, given that our single-band 1.3 mm measurement likely probes the Rayleigh-Jeans tail of emission for temperatures $\sim$100 K. Our observations probe 140–220 μm in the rest-frame. Figure 2 shows this temperature dependence. If we use the dust temperature of $\sim$114 K estimated in Casey et al. (2024), which is consistent with other independent theoretical estimates on the dust temperature (Li et al. 2024), then we can roughly place upper limits on the IR luminosity of LRDs at $< 10^{12}$ $L_\odot$ (at 3σ) for individual measurements and at $<10^{11}$ $L_\odot$ for the stack.

4. SUMMARY

We present ALMA band 6 (1.3 mm) continuum observations of a sample of 60 little red dots drawn from Akins et al. (2024). None of the LRDs have dust continuum detections; similarly, a stack of all ALMA data also results in a non-detection. The RMS of these observations, $\sim$22 μJy, places a dust mass limit for individual LRDs at $<10^7$ $M_\odot$ at 3σ and a limit of $<10^6$ $M_\odot$ at 3σ from the stack. These limits are consistent with our previous work (Casey et al. 2024) which argues that the dust mass reservoir around LRDs should be of order $\sim 10^{4-5}$ $M_\odot$ based on their compact sizes and relatively modest attenuation. If we adopt the predicted dust temperature of LRDs of $\sim$100 K from Casey et al. (2024), which is consistent with the temperature independently estimated by Li et al. (2024), we place a limit on the IR luminosity of LRDs at $\sim10^{11}$ $L_\odot$ (3σ, for the stack). We show the stacked limit in context with the average (and predicted) SED for LRDs in Figure 3.

Our results are consistent with two other literature works that placed limits on dust in LRDs in the literature: Xiao et al. (2025) present NOEMA 1.3 mm constraints for two bright $z > 7$ LRDs, and Setton et al. (2025) present multi-band ALMA follow-up of two exceptionally luminous LRDs at $z = 3-5$. Both our measurements and those in Xiao et al. (2025) and Setton et al. (2025) place the most stringent constraints on long wavelength dust emission for the population, roughly an order of magnitude deeper than previous millimeter continuum constraints from Labbe et al. (2022) and Akins et al. (2024). Our constraints are largely complimentary to the other stringent limits by constraining a large sample of 60 LRDs as opposed to very deep observations of 2 (particularly bright) LRDs each.

To-date, no LRD has been firmly identified through its millimeter emission in continuum (only one has a tentative detection of neutral gas in the millimeter; A2744-45924 at $z = 4.46$ presented in Akins et al. 2025, whose continuum limits come from Setton et al.). If predictions hold, detection via dust continuum will likely not happen without significant sensitivity upgrades to ALMA's receivers. Future far-infrared missions such as PRIMA will be able to reach deeper stacking limits at $\lambda_{\rm obs} \sim 30 - 200\,\mu$m, and may be capable of directly detecting warm dust emission in the brightest LRDs like A2744-45924.

It could be, however, that the predicted dust content might not even be there if LRDs' reddening originates from physics beyond dust-obscuration entirely. In the emerging picture that LRDs may be dominated by a population of low-mass black holes cocooned in a shroud of dense, ionized gas accreting at super-Eddington luminosities (e.g. Inayoshi & Maiolino 2024; Naidu et al. 2025; Rusakov et al. 2025; de Graaff et al. 2025), then the 'reddening' would instead be caused by at atmosphere of dense gas relatively devoid of dust. If that hypothesis holds, it logically follows that their submillimeter emission would be even less significant than the already meager predictions.

CMC thanks the National Science Foundation for support through grants AST-2009577 and AST-2307006 and to NASA through grant JWST-GO-01727 awarded by the Space Telescope Science Institute, which is operated by the Association of Universities for Research in Astronomy, Inc., under NASA contract NAS 5-26555. HBA acknowledges support from the Harrington Graduate Fellowship at UT Austin, and HBA and ORC thank the National Science Foundation for support from Graduate Research Fellowship Program awards. This project has received funding from the European Union's Horizon 2020 research and innovation programme under the Marie Skłodowska-Curie grant agreement No 101148925.

REFERENCES

Akins, H. B., Casey, C. M., Lambrides, E., et al. 2024, arXiv e-prints, arXiv:2406.10341. https://arxiv.org/abs/2406.10341

Akins, H. B., Casey, C. M., Chisholm, J., et al. 2025, arXiv e-prints, arXiv:2503.00998, doi: 10.48550/arXiv.2503.00998

Baggen, J. F. W., van Dokkum, P., Brammer, G., et al. 2024, arXiv e-prints, arXiv:2408.07745, doi: 10.48550/arXiv.2408.07745

Bisigello, L., Rodighiero, G., Fotopoulou, S., et al. 2025, arXiv e-prints, arXiv:2503.15323, doi: 10.48550/arXiv.2503.15323

Casey, C. M., Akins, H. B., Kokorev, V., et al. 2024, ApJL, 975, L4, doi: 10.3847/2041-8213/ad7ba7

Casey, C. M., Zavala, J. A., Aravena, M., et al. 2019, ApJ, 887, 55, doi: 10.3847/1538-4357/ab52ff

Casey, C. M., Kartaltepe, J. S., Drakos, N. E., et al. 2023, ApJ, 954, 31, doi: 10.3847/1538-4357/acc2bc

Chabrier, G. 2003, PASP, 115, 763, doi: 10.1086/376392

de Graaff, A., Rix, H.-W., Naidu, R. P., et al. 2025, arXiv e-prints, arXiv:2503.16600, doi: 10.48550/arXiv.2503.16600

Greene, J. E., Labbe, I., Goulding, A. D., et al. 2023, arXiv e-prints, arXiv:2309.05714, doi: 10.48550/arXiv.2309.05714

Inayoshi, K., & Maiolino, R. 2024, arXiv e-prints, arXiv:2409.07805, doi: 10.48550/arXiv.2409.07805

Ji, X., Maiolino, R., Übler, H., et al. 2025, arXiv e-prints, arXiv:2501.13082, doi: 10.48550/arXiv.2501.13082

Kocevski, D. D., Finkelstein, S. L., Barro, G., et al. 2024, arXiv e-prints, arXiv:2404.03576, doi: 10.48550/arXiv.2404.03576

Kokorev, V., Caputi, K. I., Greene, J. E., et al. 2024, arXiv e-prints, arXiv:2401.09981. https://arxiv.org/abs/2401.09981

Labbe, I., van Dokkum, P., Nelson, E., et al. 2022, arXiv e-prints, arXiv:2207.12446. https://arxiv.org/abs/2207.12446

Labbe, I., Greene, J. E., Bezanson, R., et al. 2023, arXiv e-prints, arXiv:2306.07320, doi: 10.48550/arXiv.2306.07320

Lambrides, E., Chiaberge, M., Long, A. S., et al. 2024, ApJL, 961, L25, doi: 10.3847/2041-8213/ad11ee

Li, A., & Draine, B. 2001, ApJ, 554, 778, doi: 10.1086/323147

Li, Z., Inayoshi, K., Chen, K., Ichikawa, K., & Ho, L. C. 2024, arXiv e-prints, arXiv:2407.10760, doi: 10.48550/arXiv.2407.10760

Lin, R., Zheng, Z.-Y., Jiang, C., et al. 2025a, ApJL, 980, L34, doi: 10.3847/2041-8213/adaaf1

Lin, X., Fan, X., Wang, F., et al. 2025b, arXiv e-prints, arXiv:2504.08039, doi: 10.48550/arXiv.2504.08039

Ma, Y., Greene, J. E., Setton, D. J., et al. 2025, arXiv e-prints, arXiv:2504.08032, doi: 10.48550/arXiv.2504.08032

Madau, P. 2025, arXiv e-prints, arXiv:2501.09854, doi: 10.48550/arXiv.2501.09854

Matthee, J., Naidu, R. P., Brammer, G., et al. 2024, ApJ, 963, 129, doi: 10.3847/1538-4357/ad2345

McKinney, J., Hayward, C. C., Rosenthal, L. J., et al. 2021, ApJ, 921, 55, doi: 10.3847/1538-4357/ac185f

Naidu, R. P., Matthee, J., Katz, H., et al. 2025, arXiv e-prints, arXiv:2503.16596, doi: 10.48550/arXiv.2503.16596

Oke, J. B., & Gunn, J. E. 1983, ApJ, 266, 713, doi: 10.1086/160817

Planck Collaboration, Aghanim, N., Akrami, Y., et al. 2020, A&A, 641, A6, doi: 10.1051/0004-6361/201833910

Quadri, G., Trinca, A., Lupi, A., Colpi, M., & Volonteri, M. 2025, arXiv e-prints, arXiv:2505.05556, doi: 10.48550/arXiv.2505.05556

Rusakov, V., Watson, D., Nikopoulos, G. P., et al. 2025, arXiv e-prints, arXiv:2503.16595, doi: 10.48550/arXiv.2503.16595

Setton, D. J., Greene, J. E., Spilker, J. S., et al. 2025, arXiv e-prints, arXiv:2503.02059, doi: 10.48550/arXiv.2503.02059

Taylor, A. J., Finkelstein, S. L., Kocevski, D. D., et al. 2024, arXiv e-prints, arXiv:2409.06772, doi: 10.48550/arXiv.2409.06772

Taylor, A. J., Kokorev, V., Kocevski, D. D., et al. 2025, arXiv e-prints, arXiv:2505.04609, doi: 10.48550/arXiv.2505.04609

Wang, B., de Graaff, A., Davies, R. L., et al. 2024, arXiv e-prints, arXiv:2403.02304, doi: 10.48550/arXiv.2403.02304

Williams, C. C., Alberts, S., Ji, Z., et al. 2023, arXiv e-prints, arXiv:2311.07483, doi: 10.48550/arXiv.2311.07483

Xiao, M., Oesch, P. A., Bing, L., et al. 2025, arXiv e-prints, arXiv:2503.01945, doi: 10.48550/arXiv.2503.01945